processes

MDPI

Article

A Novel Porous Ni, Ce-Doped PbO_2 Electrode for Efficient Treatment of Chloride Ion in Wastewater

Sheng Liu, Lin Gui, Ruichao Peng and Ping Yu *

College of Chemistry & Molecular Science, Wuhan University, Wuhan 430072, China; sgg520@whu.edu.cn (S.L.); lingui@whu.edu.cn (L.G.); prc@whu.edu.cn (R.P.)

* Correspondence: yuping@whu.edu.cn; Tel.: +86-027-6875-2511

Received: 29 March 2020; Accepted: 9 April 2020; Published: 16 April 2020

Abstract: The porous Ti/Sb-SnO_2/Ni-Ce-PbO_2 electrode was prepared by using a porous Ti plate as a substrate, an Sb-doped SnO_2 as an intermediate, and a PbO_2 doped with Ni and Ce as an active layer. The surface morphology and crystal structure of the electrode were characterized by scanning electron microscope(SEM), energy dispersive spectrometer(EDS), and X-Ray diffraction(XRD). The electrochemical performance of the electrodes was tested by linear sweep voltammetry (LSV), cyclic voltammetry (CV), electrochemical impedance spectroscopy (EIS), and electrode life test. The results show that the novel porous Ni-Ce-PbO_2 electrodes with larger active surface area have better electrochemical activity and longer electrode life than porous undoped PbO_2 electrodes and flat Ni-Ce-PbO_2 electrodes. In this work, the removal of Cl^- in simulated wastewater on three electrodes was also studied. The results show that the removal effect of the porous Ni-Ce-PbO_2 electrode is obviously better than the other two electrodes, and the removal rate is 87.4%, while the removal rates of the other two electrodes were 72.90% and 80.20%, respectively. In addition, the mechanism of electrochemical dechlorinating was also studied. With the progress of electrolysis, we find that the increase of OH^- inhibits the degradation of Cl^-, however, the porous Ni-Ce-PbO_2 electrode can effectively improve the removal of Cl^-.

Keywords: porous Ni-Ce-PbO_2; co-doping; active surface area; removal rate

1. Introduction

The widespread use of chlorinated compounds such as HCl, NaCl, and $MgCl_2$ in the industrial field has increased the content of chloride ion in wastewater [1,2]. If it is discharged into the water body beyond control, the water environment will be seriously damaged. The accumulation of chloride ions will make the soil salinized and alkalized, and excessive intake of chlorine by the human body will cause organ damage. Chloride ions are corrosive to pipelines, boilers, etc., and can erode buildings and reduce durability of the concrete structure. For example, a large amount of Cl^- in desulfurization wastewater discharged from thermal power plants can corrode pipelines and equipments [3].

At present, the most widely used method for treating Cl^- in wastewater is chemical precipitation [4]. However, the concentration of Cl^- in the treated wastewater is still high. The treatment of chloride ion in wastewater by chemical precipitation will be limited in the future [5]. How to treat desulfurization wastewater in depth, meet the discharge requirements, and reduce the impact on the environment has always been a difficult problem in the field of wastewater treatment at home and abroad. Therefore, advanced oxidation processes (AOPs) [6,7] such as catalytic ozonation, Fenton oxidation, supercritical water oxidation, electrochemical oxidation, photocatalytic oxidation, etc., [8] have been studied. Electrochemical oxidation is one of the most eye-catching AOPs. It has the advantages of good treatment effect, small floor area, high degradation efficiency, short residence time and no secondary pollution, and has broad application prospects in the advanced treatment of salt compounds and

organic compounds [9]. In the recent years, electrochemical oxidation technology has been increasingly studied for the treatment of chloride ion in wastewater [10].

The degradation efficiency and degradation products of electrochemical oxidation process change with the anode material [11], which means that anode material is one of the main factors in electrochemical oxidation process [12,13]. Because of the critical role of anode materials, scholars have been studying new anodes for many years [14]. The earliest graphite and carbon electrodes have the disadvantages of low current efficiency and poor mechanical strength [15]. Subsequently, metal anodes were developed. At present, metal oxide electrode is widely used and its preparation process is mature, such as dimensionally stable anode (DSA) (e.g., RuO_2, IrO_2, PbO_2, SnO_2) [11]. With the deepening of research, 3D porous structure compounds are widely used in the preparation of anode materials because of their large specific surface area, such as carbon nanotubes (CNT), porous graphene (GE), etc., [16,17], which can significantly change the structure of the coating when doped in the metal oxide coating [11]. Scholars have found that doping metal elements in metal oxide coatings can significantly improve the electrode activity and extend service life [18], such as Ce, Bi, Fe, Co, etc., [11]. In addition, it has been found that many rare earth oxides doped into PbO_2 can significantly improve the electrochemical performance of the electrode [19]. Kong et al. reported that doping Er_2O_3, Gd_2O_3, La_2O_3, and Ce_2O_3 on PbO_2 electrode could promote the degradation of 4-chlorophenol [20]. Jin et al. [20] found that doping Ce can form smaller crystal size on the surface of the electrode, resulting in the increase of specific surface area and catalytically active sites. Xia et al. [21] reported that proper doping of Ni can make the grains dense, which not only facilitates electron movement, and improves electrochemical performance, but also helps to extend electrode life.

In this work, we intended to use a porous Ti plate as the substrate, because the porous structure has large specific surface area. We can improve the electrochemical activity and stability of the electrode by doping Ce and Ni in the active layer PbO_2 electrode [22]. The doping of Ce and Ni reduces the crystal size of the active layer [11,21], but increases the surface area of the active layer and the electrochemical activity of the electrode, in addition, the service life of the electrode is extended to some extent. Finally, the electrochemical activity and stability of porous Ni-Ce-PbO_2 electrodes were investigated and compared with the conventional porous undoped PbO_2 electrode and the doped flat Ni-Ce-PbO_2 electrode. In this experiment, simulated wastewater with high chlorine content was selected as the target pollutant. The electrochemical performance of the electrode was investigated by comparing the effects of three kinds of electrodes on the treatment of chloride ions in simulated wastewater.

2. Experimental

2.1. Materials

Porous titanium plate with a purity of 99.9% was purchased from Baoji Jinkai Technology Co., Ltd., Jinan, China. $Ni(NO_3)_2$ $6H_2O$ was purchased from Xiqiao Chemical Co. Ltd., Foshan, China. All other chemicals were purchased from Sino pharm Chemical Reagent Co. Ltd., Shangai, China. All chemicals were of analytical grade and used as received. In this work, deionized water was used in all solutions.

2.2. Electrode Preparation

2.2.1. Titanium Surface Preparation

The porous titanium plates (20 mm × 10 mm × 2.8 mm) bought by Baoji Jinkai Technology Co., Ltd., Jinan, China, had a purity of 99.9% and an average pore diameter of 50 μm to pretreat the substrate. The porous titanium plate was ultrasonically cleaned in acetone for 15 min, washed in 20% NaOH solution at 90 °C for 1 h, and etched in a 15 wt % oxalic acid solution at 90 °C for 1 h until a gray matte titanium matrix was formed, and finally saved in ethanol.

The surface treatment of the flat titanium plate (20 mm × 10 mm × 2.8 mm) is similar to porous titanium plate.

2.2.2. Coating SnO_2–Sb_2O_3

The electrode intermediate layer was prepared by thermal decomposition method [11]. Total of 1.2 g $SnCl_4$, 0.2 g Sb_2O_3, and 10 mL concentrated hydrochloric acid were dissolved in 25 mL of isopropanol to obtain a precursor-coating solution. The solution was colorless, transparent, slightly sticky. Then the pretreated porous titanium plate was immersed in the precursor solution. After soaking, it was taken out and dried in an oven at 110 °C, and then calcined in a muffle furnace at 500 °C for 15 min. After cooling the plate, the drying and calcining process was repeated several times, and the high-temperature baking time in the last time was extended to 1 h to obtain a porous Ti/Sb-SnO_2 electrode. The main purpose of this layer is to improve the conductivity of the electrode and prevent the titanium matrix from being oxidized to form TiO_2.

The precursor solution can be directly brushed on the surface of the flat titanium plate with a brush. Other preparation processes of the intermediate layer of the flat electrode are similar to that of the porous electrode.

2.2.3. Electrochemical Deposition Ni–Ce–PbO_2

$Pb(NO_3)_2$, $Ni(NO_3)_2$, and $Ce(NO_3)_2$ were dissolved in 250 mL water at a ratio of 100:1:1 of Pb, Ni, and Ce. Then, 0.04 M NaF and 4 mL/L of PTFE were added, before adding 0.1 mol/L HNO_3 to adjust the pH to 1, to form an electrodeposition solution. The control temperature was 65 °C, the current density was 20 mA/cm^2, the electrodeposition time was 1 h, so as to deposit a surface layer of lead dioxide with Ce, Ni co-doped on the surface of the intermediate layer tin antimony oxide, that is, porous Ti/Sb-SnO_2/Ni-Ce-PbO_2 electrode.

In addition to the raw materials (Ni $(NO_3)_2$ and Ce $(NO_3)_2$), the preparation process of porous PbO_2 electrode is similar to that of porous Ni-Ce PbO_2 electrode

2.3. Electrode Characterization

The surface morphology was observed using a scanning electron microscope (Quanta 200 of FEI, Hillsboro, OR, USA). X-ray diffraction (XRD) patterns of samples were obtained with an X-ray diffractometer (PANalytical, Almelo, The Netherlands). Cyclic voltammetry (CV), linear sweep voltammetry (LSV), and electrochemical impedance spectroscopy (EIS) were performed at room temperature using a computer-controlled electrochemical workstation (CHI 660E, CH Instruments, Shanghai, China) with a conventional three-electrode system. The prepared PbO_2-based electrode (20 mm × 20 mm) was used as the working electrode, a saturated Ag/AgCl electrode was employed as the reference electrode, and a stainless steel sheet was applied as the counter electrode. All potentials were referred to the SCE. The stability tests (up to 20 h) were performed by the accelerated life test with a current density of 1 A·cm^{-2} and a temperature of 60 °C in 2 M H_2SO_4 solution for porous undoped PbO_2 electrodes, porous Ni-Ce–PbO_2 electrodes, and Flat Ni-Ce–PbO_2 electrodes. These tests were performed in a three-electrode system.

2.4. Electrochemical Oxidation

A simulated chlorine-containing wastewater with a chloride ion concentration of 4 g/L and a volume of 200 mL was selected as the experimental wastewater; the temperature was 298 K in all experiments. The electrochemical oxidation experiment was conducted by a batch method, and the device was mainly composed of a DC power source, a collector types magnetic stirrer, and a glass reactor. The anode (PbO_2-based electrodes) and the cathode (flat titanium plate) were placed parallel to each other and perpendicular to the solution level with a distance of 1 cm. The volume of simulated wastewater in all experiments was 200 mL and the Cl^- concentration was 4 g/L. The temperature of all experiments was maintained at 298 K. All pH values in the experiment were determined by a pH meter and all Cl^- concentration in the experiment were determined by titration with a standard $AgNO_3$ solution.

3. Results and Discussion

3.1. Surface Morphological and Crystallographic Analysis

The SEM images of the plate-modified Ni-Ce-PbO_2 electrode, the porous undoped PbO_2 electrode, and the porous Ni-Ce-PbO_2 electrode are shown in Figure 1. It can be seen that the porous undoped PbO_2 electrode and the porous Ni-Ce-PbO_2 electrode still have many small holes in the electrode surface while compared with porous Ti plate (Figure 1a), indicating that the PbO_2 coating did not block the porous structure. From Figure 1b,f it can be seen that the porous Ni-Ce-PbO_2 electrodes apparently have larger pores and specific surface area compared to the flat Ni-Ce-PbO_2 electrodes.

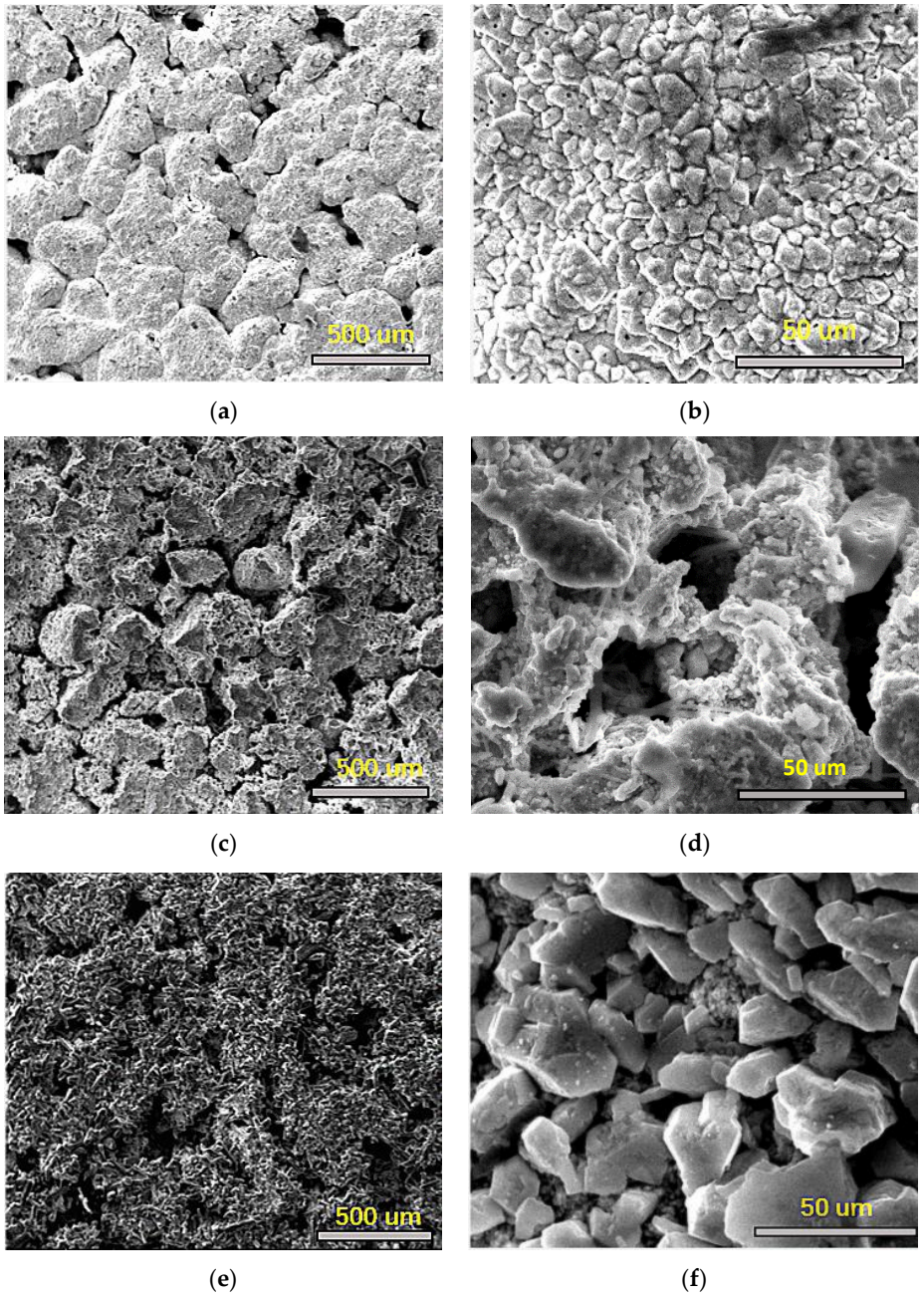

Figure 1. SEM of different electrodes, (**a**) (porous titanium plate, 80×); (**b**) (flat Ni-Ce-PbO_2 electrode, 1200×) and (**c**) (porous undoped PbO_2 electrode, 80×); (**d**) (porous undoped PbO_2 electrode, 1200×) and (**e**) (porous Ni-Ce-PbO_2 electrode, 80×); (**f**) (porous Ni-Ce-PbO_2 electrode, 1200×).

The porous PbO_2 electrode doped with Ni and Ce (Figure 1e,f) can make the holes smaller or bigger on the surface of the electrodes, and the specific surface area was larger than porous undoped PbO_2 electrodes (Figure 1c,d). Besides, the EDS spectrum of different PbO_2 electrodes is shown in Figure 2a, which confirms that there are O, Pb, Ce, Ni elements in the porous Ni-Ce-PbO_2 electrode, while there are only O and Pb elements in the porous undoped PbO_2 electrodes. Thus, it can be concluded that the Ni and Ce was successfully doped into the PbO_2 films and doping of Ni and Ce can reduce the grain size of the PbO_2 coating.

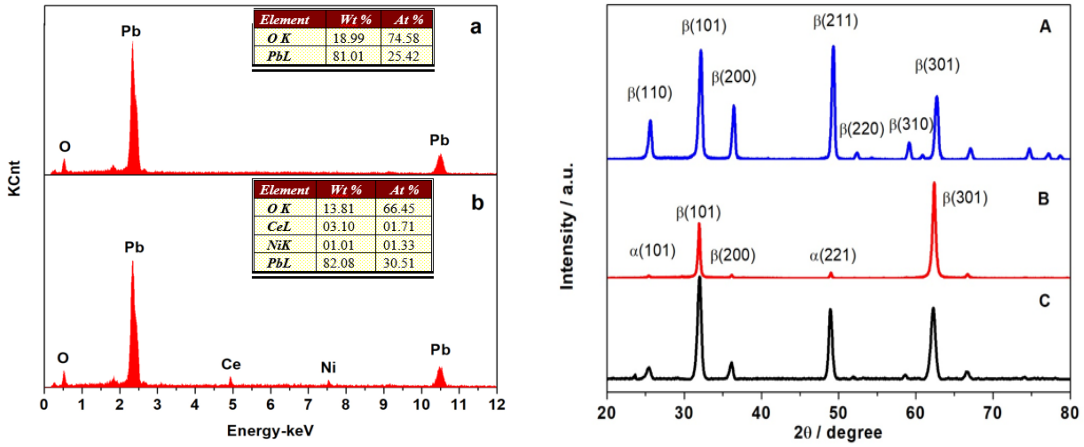

(**a**) (**b**)

Figure 2. (**a**) EDS of a (porous PbO_2 electrode) and b (porous Ni-Ce-PbO_2 electrode); (**b**) XRD diffraction patterns of different Electrodes A (Porous Ti/Sb-SnO_2/PbO_2 electrode), B (Porous Ti/Sb-SnO_2/Ni-Ce-PbO_2 electrode), and C (Standard XRD pattern of PbO_2).

From Figure 2b, it can be seen that the diffraction peaks of undoped porous show that dioxide electrodes appear at 25.4 degrees, 31.9 degrees, 36.1 degrees, 48.9 degrees, 58.8 degrees, 62.4 degrees, and 66.8 degrees, which are consistent with the JCPDS card (41–1492) in pattern, indicating that the main component of undoped PbO_2 surface layer is β-PbO_2 and the coating of porous Ni-Ce-PbO_2 electrode consists of a mixture of crystalline phases of α and β-PbO_2. The content of α-PbO_2 is higher than that of undoped PbO_2 because the doping of Ce changes the preferred crystalline orientation of the electrode surface and forms smaller grains. In addition, compared with the undoped PbO_2, the intensity of the diffraction peaks of Ni-Ce-PbO_2 decreases or even disappears because of the doping of Ni and Ce. The reason may be that doping of Ni and Ce changes the nucleation and growth of crystals in the coating, making the electrode have smaller crystal size than the undoped PbO_2 electrode, which can also be seen from the SEM image. The average crystallite size calculated from the width of [101] diffraction peaks by Scherrer's formula is 17.64 nm (Ce–Ni) and 28.76 nm (undoped). According to literature [20], the diffraction peak width is inversely proportional to the crystallite size. The result indicates that the deposited Ni-Ce-PbO_2 has smaller crystallite size than other electrode. Smaller crystal size may help to form larger specific surface area which may lead to better electrochemical performance.

3.2. Electrochemical Performance Test

As shown in Figure 3a, no redox peak signal was observed on any of the electrodes in the blank Na_2SO_4 solution, indicating that PbO_2 is an electrochemically inert material in the blank Na_2SO_4 solution. After the addition of Cl^- (Figure 3b), a distinct oxidation peak was obtained. There is no doubt that the oxidation peak is attributed to the oxidation of Cl^- on the surface of the anode. However, no corresponding reduction peak was observed in the reverse scanning from 3 V to 0 V, indicating that the oxidation of Cl^- is a completely irreversible electrode reaction process. The oxidation peak potential of the porous Ni-Ce-PbO_2 electrode (2.01 V vs. SCE) was lower than that of the other two electrodes

(2.24 and 2.48 V), but the oxidation peaks current (0.031 A) was significantly higher than the other two electrodes (0.028 A and 0.024 A), which showed that the porous Ni-Ce-PbO_2 electrode has higher electro-catalytic activity for Cl^-, and the improvement of its electro-catalytic activity is not only related to the increase in electrode surface area caused by its porous structure and doping with Ni and Ce, but also due to changes in the PbO_2 band structure. The electrode doping Ni and Ce not only increases the donor area of PbO_2, but also increases the donor level of PbO_2, making it easier for electrons to jump from the donor level to the conduction band [21]. Therefore, the conductivity of PbO_2 is improved.

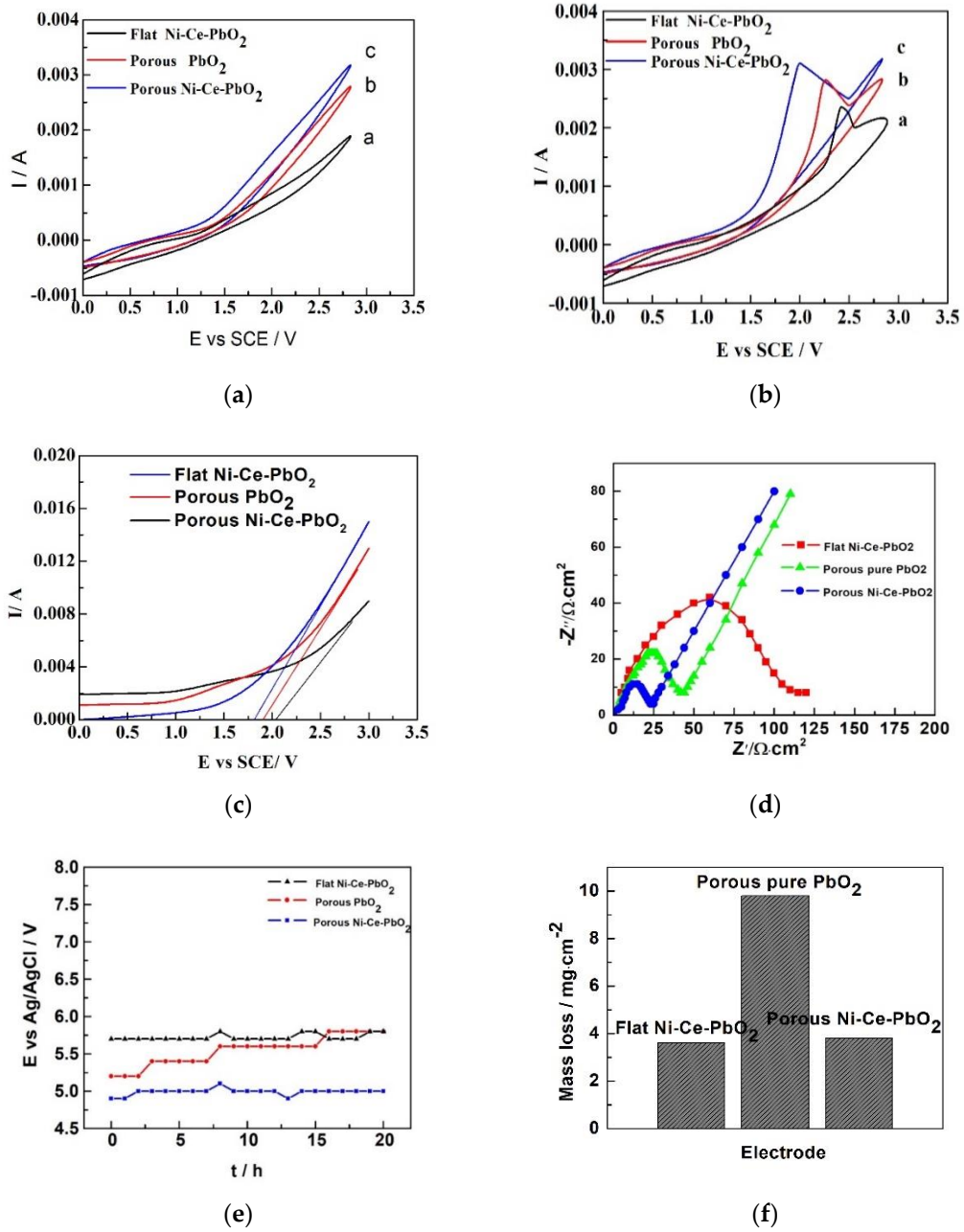

Figure 3. (**a**) Cyclic voltammetry (CV) of different PbO_2 electrodes measured in 0.1mol·L^{-1} Na_2SO_4 solution, (**b**) 0.1 mol·L^{-1} Na_2SO_4 solution (pH = 6.5) containing 4 g L^{-1} Cl^-, scan rate: 50 mV s^{-1}, T = 298 K, (**c**) LSV curves of different electrodes measured in 0.5 M Na_2SO_4, scan rate: 10 mV s^{-1}, T = 298 K, (**d**) EIS of different electrodes. Conditions: T = 298 K; [H_2SO_4] = 1 M. (**e**) Electrode stability tests: electrode potential vs. time for the electrolysis using different electrodes. (**f**) The mass losses of electrodes after accelerated life tests for 20 h.

The oxygen evolution overpotential (OEP) of different electrodes could be measured by LSV. According to the polarization curve in Figure 3c, the OEP of the porous Ni-Ce-PbO_2 electrode was the highest with 2.09 V (vs. SCE) compared with the flat Ni-Ce-PbO_2 electrode of 1.81 V (vs. SCE) and the porous PbO_2 electrode of 1.91 V (vs. SCE), respectively. The electrodes with high OEP values can produce more hydroxyl radicals [23]. In addition, it can be seen from Figure 3c that the porous Ni-Ce-PbO_2 electrodes had higher oxygen evolution current than the other two electrodes. The higher oxygen releases current also verified that the active surface area of the porous Ni-Ce-PbO_2 electrode is larger than that of the other PbO_2-based electrodes.

In Figure 3d, there is an obvious semicircle in the electrochemical impedance spectroscopy (EIS) of the three electrodes. The radius of the semicircle usually reflects the magnitude of the transfer resistance R_{ct} of the chlorine evolution or oxygen evolution reaction, which is available from the EIS spectrum. The R_{ct} sizes of Ni-Ce-PbO_2 electrodes, porous PbO_2 electrodes, and porous Ni-Ce-PbO_2 electrodes were 59.4, 21.2, and 12.2, respectively. It is indicated that the porous Ni-Ce-PbO_2 electrode has the best conductivity, the most active surface sites, and the highest chlorine evolution activity.

The service life is a critical factor in the practical application of the electrode. Under the condition of anode current of 1A pa^{-2} and temperature of 60 °C, the accelerated life test of different PbO_2 electrodes was carried out in 2M H_2SO_4 solution for 20 h. According to Figure 3e,f, the Ni-Ce-PbO_2 electrode exhibited better electrochemical stability and less mass loss than the pure PbO_2 electrode. It is well-known that the main reasons of mass loss of electrode are the separation and dissolution of PbO_2 film, and the mass loss is proportional to the service life of the electrode. Therefore, it can be concluded that the stability of Ni-Ce-PbO_2 electrode is much better than that of pure PbO_2 electrode by the modification of Ni and Ce. The mass loss of the porous Ni-Ce-PbO_2 electrode is slightly larger than that of the flat Ni-Ce-PbO_2, mainly because of the loose porosity of the structure. In fact, in the experiments, we found that film peeled off on the pure PbO_2 electrode, but not on the other two modified PbO_2 electrodes.

3.3. Electrochemical Oxidation of Cl^- in Simulated Wastewater

The electrochemical oxidation of simulated wastewater was compared with three kinds of electrodes. From Figure 4a, after electrolysis for 100 min, the removal rate of Cl^- on the porous Ni-Ce-PbO_2 electrode was as high as 87.4%. At the same time, the plate Ni-Ce-PbO_2 electrode and the porous PbO_2 electrode were used as anodes, and the highest removal rates of Cl^- were 72.90% and 80.20%, respectively. Obviously, the above results show that the electrochemical oxidation ability of the porous Ni-Ce-PbO_2 electrode was much higher than the other two electrodes. This may be due to the fact that the porous structure increases the surface area of the electrode and the doping of Ni and Ce further increases the surface area of the electrode, which facilitates the adsorption of Cl^- on the surface of the anode and promotes the mass transfer and exchange of the reactants. Thus, the electrochemical oxidation ability of the electrode is improved. As is shown in Figure 4b that in the early stage of electrolysis, the removal rate of Cl^- was higher than that in the later stage because of the enrichment of Cl^- in wastewater. The results show that higher current density result in higher Cl^- removal rate, and the difference in Cl^- removal rate was not obvious at relatively higher current densities. With the progress of electrolysis, the decrease of Cl^- concentration inhibited the oxidation of Cl^- and reached equilibrium at a certain time, in which Cl^- cannot be completely removed. However, the porous Ni-Ce-PbO_2 electrode with large specific surface area can effectively improve the removal rate of Cl^-. During the process of degradation of Cl^-, the chlorine evolution reaction and oxygen evolution side reaction in the anode proceed simultaneously, the content of Cl^- is higher and the content of OH^- is lower in the initial stage of reaction process (Figure 4c). The reaction formulas are as follows:

$$\text{Anode: } 2Cl^- \rightarrow Cl_2 + 2e^- \quad (1)$$

$$Cl_2 + 2H_2O \rightarrow HClO + H_3O^+ + Cl^- \quad (2)$$

$$HClO + H_2O \rightarrow H_3O^+ + ClO^- \quad (3)$$

$$\text{Cathode: } H_2O \rightarrow H^+ + OH^- \quad (4)$$

$$2H^+ + 2e^- \rightarrow H_2 \quad (5)$$

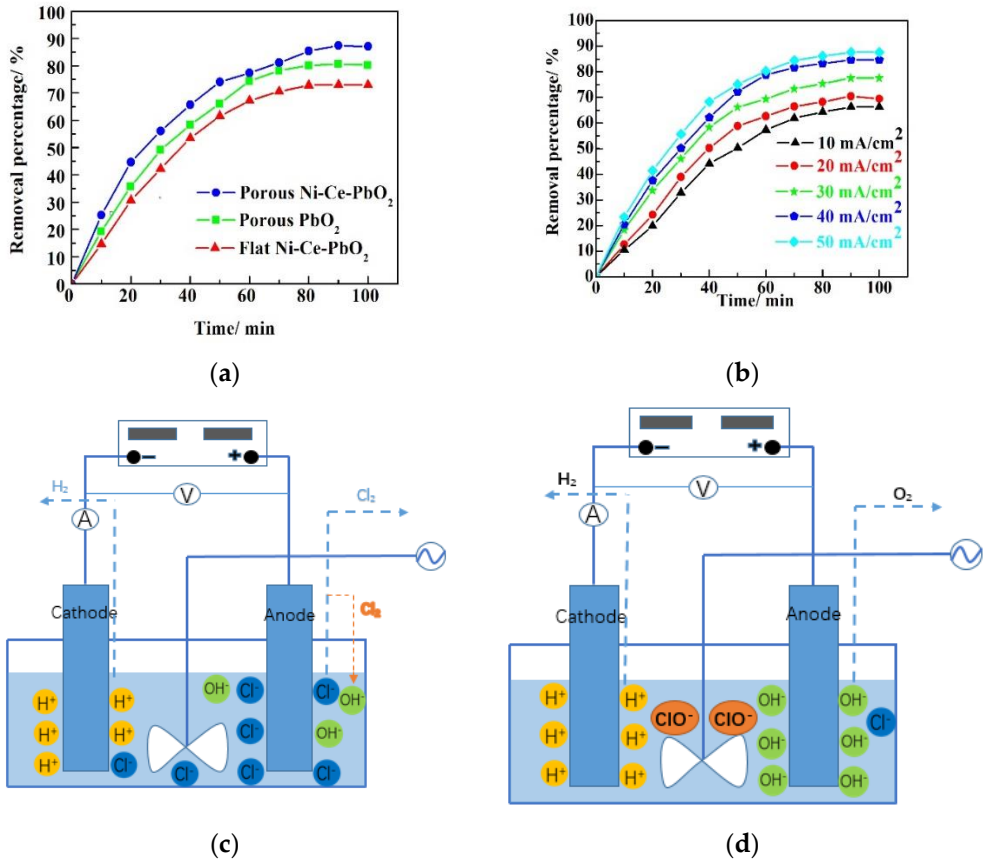

Figure 4. (**a**) Variation of Cl^- removal percentage with time during electrochemical oxidation on different electrodes, conditions: current density = 50 mA/cm^2; T = 298 K; [Cl^-] = 4 g/L, (**b**) at different current densities, conditions: porous Ni-Ce-PbO_2 electrode; T = 298 K; [Cl^-] = 4 g/L and electrochemical reaction process of electrode dechlorinating (**c**) at 30 min and (**d**) at 100 min.

According to the investigation [24], under the experimental conditions, the anode mainly generates Cl_2 (Equation (1)). The cathode produces a large amount of OH^-, which exists in the solution to raise the pH of the solution quickly, except a small portion is transferred to the anode for consumption. The increase of OH^- concentration promotes the disproportionation of chlorine and forms a large number of ClO^- (Equations (2) and (3)). In addition, Figure 4a also shows the fact that the Cl^- removal rate increases significantly with the increase of the initial concentration. But after the electrolysis time reaches 90 min, a large amount of Cl^- is removed and the OH^- concentration in the solution is gradually increased. This can also be seen from Figure 4c,d, the reaction formulas are as follows:

$$\begin{gathered} H_2O \rightarrow H^+ + OH^- \\ \text{Anode: } 2OH^- - 4e^- \rightarrow O_2 + 2H^+ \\ \text{Cathode: } 4H^+ + 4e^- \rightarrow 2H_2 \end{gathered} \quad (6)$$

A large amount of OH groups accumulates on the surface of the anode, which hinders the contact between a small amount of Cl^- in the solution and the anode, so that the oxygen evolution reaction on the surface of the anode gradually becomes the main reaction. The consumption of OH^- on the anode results in a small part of residual Cl^- in the solution which cannot be removed, and another

small part of Cl^- is converted into ClO^- and HClO [24] (Equations (1)–(3)), which greatly limits the removal of Cl^-. Also as a DSA electrode, the porous Ni-Ce-PbO_2 electrode degraded 87.4% of Cl^- at 90 min because of its large active surface area, while the degradation rate of the plated Ni-Ce-PbO_2 electrode and the porous PbO_2 electrode were only 72.90% and 80.20%, respectively. Therefore, the porous Ni-Ce-PbO_2 electrode breaks through the limitation of the conventional electrode in removing Cl^-. In addition, we also detected the concentration of Pb^{2+} and Ni^{2+} in the solution after the 5th oxidation, and found that the concentration of Pb^{2+} was only about 0.0085 mg/L, and Ni^{2+} was even less, far lower than the standard of the World Health Organization. It shows that it is environment friendly and will not cause secondary pollution.

4. Conclusions

In this paper, porous Ni-Ce-doped PbO_2 electrodes were successfully prepared on a porous titanium substrate by thermal deposition and electrodeposition. The surface morphology, crystal structure, electrochemical activity, and electrode stability of the flat Ni-Ce-PbO_2, porous undoped PbO_2, and porous Ni-Ce-PbO_2 were tested, and the electro-catalytic properties of these three electrodes in simulated wastewater were compared.

The porous Ni-Ce-PbO_2 electrodes possessed porous structure and smaller grain size than the other two electrodes. The doping of Ni and Ce can change the nucleation and growth of crystals on the surface of the electrode, making the electrode have smaller particles, larger electrochemical active surface area, and better electrode life.

At a current density of 50 mA, the porous Ni-Ce-PbO_2 electrode was used to treat Cl^- in the simulated wastewater. The removal rate was as high as 87.4%, while the highest removal rates of the porous pure PbO_2 electrode and the flat Ni-Ce-PbO_2 electrode were 72.90% and 80.20%, respectively.

In addition, in the later stage of Cl^- oxidation, because of the increase of pH of the electrolyte, oxygen evolution reaction mainly occurs in the anode, which results in a part of Cl^- that cannot be removed from the solution and the other part that dissolves in the solution in the form of ClO^- and HClO; removal rate of Cl^- is restricted. The novel porous Ni-Ce-PbO_2 electrodes can effectively improve the removal of Cl^- because of its greater electrochemically active surface area.

Author Contributions: S.L. and P.Y. conceived and designed the experiments; S.L., L.G., and R.P. performed the experiments; S.L. analyzed the data and wrote the paper; S.L. and P.Y. revised the manuscript. All authors have read and agreed to the published version of the manuscript.

Funding: This research received no external funding.

Conflicts of Interest: The authors declare no conflict of interest.

References

1. Guàrdia, M.D.; Guerrero, L.; Gelabert, J.; Gou, P.; Arnau, J. Sensory characterisation and consumer acceptability of small calibre fermented sausages with 50% substitution of NaCl by mixtures of KCl and potassium lactate. *Meat Sci.* **2008**, *80*, 1225–1230. [CrossRef] [PubMed]
2. Xia, J.; Liu, Q.F.; Mao, J.H.; Qian, Z.H.; Jin, S.J.; Hu, J.Y.; Jin, W.L. Effect of environmental temperature on efficiency of electrochemical chloride removal from concrete. *Constr. Build. Mater.* **2018**, *193*, 189–195. [CrossRef]
3. Yang, B.; Chen, Z.; Zhang, M.; Zhang, H.; Zhang, X.; Pan, G.; Zou, J.; Xiong, Z. Effects of elevated atmospheric CO_2 concentration and temperature on the soil profile methane distribution and diffusion in rice-wheat rotation system. *J. Environ. Sci. (China)* **2015**, *32*, 62–71. [CrossRef] [PubMed]
4. Gupta, V.K.; Ali, I.; Saleh, T.A.; Nayak, A.; Agarwal, S. Chemical treatment technologies for waste-water recycling—An overview. *RSC Adv.* **2012**, *2*, 6380–6388. [CrossRef]
5. Hu, S.; Ding, S.F.; Fan, Z.S. Zero release technology of desulfurization waste water in coal—Fired power plant. *Clean Coal Technol.* **2015**, *21*, 129–133.
6. Liu, H.; Liu, Y.; Zhang, C.; Shen, R. Electrocatalytic oxidation of nitrophenols in aqueous solution using modified PbO_2 electrodes. *J. Appl. Electrochem.* **2008**, *38*, 101–108. [CrossRef]

7. Deng, Y.; Zhao, R. Advanced Oxidation Processes (AOPs) in Wastewater Treatment. *Curr. Pollut. Rep.* **2015**, *1*, 167–176. [CrossRef]
8. Shmychkova, O.; Luk'yanenko, T.; Velichenko, A.; Meda, L.; Amadelli, R. Bi-doped PbO_2 anodes: Electrodeposition and physico-chemical properties. *Electrochim. Acta* **2013**, *111*, 332–338. [CrossRef]
9. Xu, M.; Wang, Z.; Wang, F.; Hong, P.; Wang, C.; Ouyang, X.; Zhu, C.; Wei, Y.; Hun, Y.; Fang, W. Fabrication of cerium doped Ti/nanoTiO_2/PbO_2 electrode with improved electrocatalytic activity and its application in organic degradation. *Electrochim. Acta* **2016**, *201*, 240–250. [CrossRef]
10. Shuangchen, M.; Jin, C.; Gongda, C.; Weijing, Y.; Sijie, Z. Research on desulfurization wastewater evaporation: Present and future perspectives. *Renew. Sustain. Energy Rev.* **2016**, *58*, 1143–1151. [CrossRef]
11. Duan, X.; Zhao, Y.; Liu, W.; Chang, L.; Li, X. Electrochemical degradation of p-nitrophenol on carbon nanotube and Ce-modified-PbO_2 electrode. *J. Taiwan Inst. Chem. Eng.* **2014**, *45*, 2975–2985. [CrossRef]
12. Dai, Q.; Xia, Y.; Chen, J. Mechanism of enhanced electrochemical degradation of highly concentrated aspirin wastewater using a rare earth La-Y co-doped PbO_2 electrode. *Electrochim. Acta* **2016**, *188*, 871–881. [CrossRef]
13. Xia, Y.; Dai, Q.; Chen, J. Electrochemical degradation of aspirin using a Ni doped PbO_2 electrode. *J. Electroanal. Chem.* **2015**, *744*, 117–125. [CrossRef]
14. Yao, Y.; Teng, G.; Yang, Y.; Huang, C.; Liu, B.; Guo, L. Electrochemical oxidation of acetamiprid using Yb-doped PbO_2 electrodes: Electrode characterization, influencing factors and degradation pathways. *Sep. Purif. Technol.* **2019**, *211*, 456–466. [CrossRef]
15. Elaissaoui, I.; Akrout, H.; Grassini, S.; Fulginiti, D.; Bousselmi, L. Effect of coating method on the structure and properties of a novel PbO_2 anode for electrochemical oxidation of Amaranth dye. *Chemosphere* **2019**, *217*, 26–34. [CrossRef] [PubMed]
16. Xu, F.; Chang, L.; Duan, X.; Bai, W.; Sui, X.; Zhao, X. A novel layer-by-layer CNT/PbO_2 anode for high-efficiency removal of PCP-Na through combining adsorption/electrosorption and electrocatalysis. *Electrochim. Acta* **2019**, *300*, 53–66. [CrossRef]
17. Zhou, X.; Liu, S.; Yu, H.; Xu, A.; Li, J.; Sun, X.; Shen, J.; Han, W.; Wang, L. Electrochemical oxidation of pyrrole, pyrazole and tetrazole using a TiO_2 nanotubes based SnO_2-Sb/3D highly ordered macro-porous PbO_2 electrode. *J. Electroanal. Chem.* **2018**, *826*, 181–190. [CrossRef]
18. Santos, J.E.L.; de Moura, D.C.; da Silva, D.R. Application of TiO_2-nanotubes/PbO_2 as an anode for the electrochemical elimination of Acid Red 1 dye. *J. Solid State Electrochem.* **2018**, *23*, 351–360. [CrossRef]
19. Du, H.; Duan, G.; Wang, N.; Liu, J.; Tang, Y.; Pang, R.; Chen, Y.; Wan, P. Fabrication of Ga_2O_3–PbO_2 electrode and its performance in electrochemical advanced oxidation processes. *J. Solid State Electrochem.* **2018**, *22*, 3799–3806. [CrossRef]
20. Jin, Y.; Wang, F.; Xu, M.; Hun, Y.; Fang, W.; Wei, Y.; Zhu, C.G. Preparation and characterization of Ce and PVP co-doped PbO_2 electrode for waste water treatment. *J. Taiwan Inst. Chem. Eng.* **2015**, *51*, 135–142. [CrossRef]
21. Wang, Z.; Xu, M.; Wang, F.; Liang, X.; Wei, Y.; Hu, Y.; Zhu, C.G.; Fang, W. Preparation and characterization of a novel Ce doped PbO_2 electrode based on NiO modified Ti/TiO_2NTs substrate for the electrocatalytic degradation of phenol wastewater. *Electrochim. Acta* **2017**, *247*, 535–547. [CrossRef]
22. Yao, Y.; Huang, C.; Yang, Y.; Li, M.; Ren, B. Electrochemical removal of thiamethoxam using three-dimensional porous PbO_2-CeO_2 composite electrode: Electrode characterization, operational parameters optimization and degradation pathways. *Chem. Eng. J.* **2018**, *350*, 960–970. [CrossRef]
23. Xie, R.; Meng, X.; Sun, P.; Niu, J.; Jiang, W.; Bottomley, L.; Li, D.; Chen, Y.; Crittenden, J. Electrochemical oxidation of ofloxacin using a TiO_2-based SnO_2-Sb/polytetrafluoroethylene resin-PbO_2 electrode: Reaction kinetics and mass transfer impact. *Appl. Catal. B Environ.* **2017**, *203*, 515–525. [CrossRef]
24. Neodo, S.; Rosestolato, D.; Ferro, S.; De Battisti, A. On the electrolysis of dilute chloride solutions: Influence of the electrode material on Faradaic efficiency for active chlorine, chlorate and perchlorate. *Electrochim. Acta* **2012**, *80*, 282–291. [CrossRef]